Supplementary Information for:

Suppressed Surface Dynamics of Poly (methyl methacrylate) Chains in the Corona of Collapsed Dry Micelles Tethered by a Fluorinated Block Core

Biao Zuo, Wanglong Liu, Hao Fan, Yizhi Zhang , Tingting He, Xinping Wang*

Department of Chemistry, Key Laboratory of Advanced Textile Materials and Manufacturing Technology of the Education Ministry, Zhejiang Sci-Tech University, Hangzhou 310018, China.

* Email: wxinping@yahoo.com or wxinping@zstu.edu.cn

Section 1: Calculations of the number of FMA units (*n*) of $PMMA_{430}$-ec-$PFMA_n$

Since the contents of FMA were very low in the polymers, the molecular weight difference between the macroinitiator ($PMMA_{430}$) and its fluorinated polymer could not be determined by GPC. The low FMA content and the intrinsic association of the FMA units also made it inaccurate to use ^1H NMR to determine the fluorinated content. Thus, fluorine elemental analysis was employed to measure fluorinated monomer content. The number of FMA units (*n*) in $PMMA_{430}$-ec-$PFMA_n$ was calculated according to the following equation:

$$W_F\,(\%) = (17 \times 19 \times n) / (M_{430,MMA} + 532 \times n)$$

where $W_F(\%)$ is the fluorine content of copolymer measured by fluorine element analysis using the ignition method; *n* is the number of FMA units. Each fluorinated monomer FMA contains 17 fluorine atoms, and the fluorine atomic weight is 19. $M_{430,MMA}$ is the molecular weight of the $PMMA_{430}$ as measured by GPC. The molecular weight of the fluorinated monomer FMA is 532.

Section 2: Micelle size measurement of $PMMA_{430}$-ec-$PFMA_n$ in toluene by dynamic light scattering (DLS)

Dynamic light scattering (DLS) is used to measure the size and size distribution of the $PMMA_{430}$-ec-$PFMA_n$ aggregates in toluene. It can be seen that the fluorinated PMMAs with *n* ranging from 2 to 22 all form aggregates in toluene (Figure S1). When the solvophobic PFMA segment is short (*n* = 2, 4), the formed aggregates are

very loose with larger diameter (~260nm) and broad distribution. As the length of the PFMA segment increased (n = 7, 12, 22), the micelles diameter become smaller and the size distribution of the micelles also shows an apparent narrowing, which indicates the formation of more compact micelles.

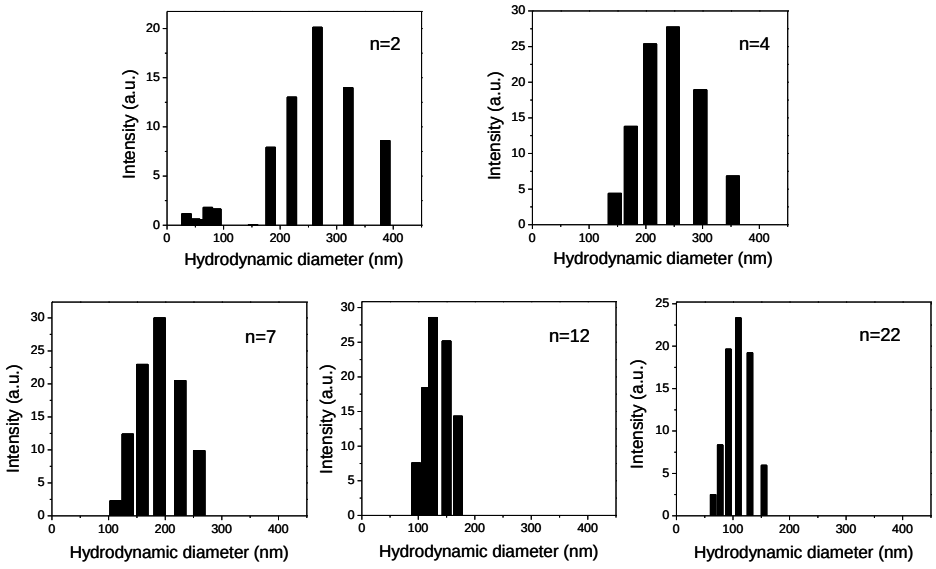

Figure S1. Size and size distribution of micelles formed by $PMMA_{430}$-ec-$PFMA_n$ in toluene with n in $PMMA_{430}$-ec-$PFMA_n$ ranging from 2 to 22 measured by dynamic light scattering (DLS).

Section 3: Transmission electron microscope (TEM) images of $PMMA_{430}$-ec-$PFMA_n$ films

The solid-state aggregative morphologies of fluorinated PMMA are characterized by JSM-2100 transmission electron microscopy (TEM) at an accelerating voltage of 200 kV, whereby a small drop of sample solution was deposited onto a carbon-coated copper EM grid (200 mesh) and dried at the room temperature and atmospheric pressure. The resultant TEM images of

$PMMA_{430}$-ec-$PFMA_n$ thin film are displayed in Figure S2. It is illustrated that the fluorinated PMMA chains with low amounts of FMA units (n = 2, 4) homogeneously distribute within the film bulk without preferential aggregation. Upon increase of n to 7, some loose-packed, larger "micelle-like" aggregations are formed inside the film, with wide size distribution. For $PMMA_{430}$-ec-$PFMA_{12}$ and $PMMA_{430}$-ec-$PFMA_{22}$, TEM reveals some size-uniform spherical aggregates formed in the films. The TEM results are readily consistent with the AFM observations.

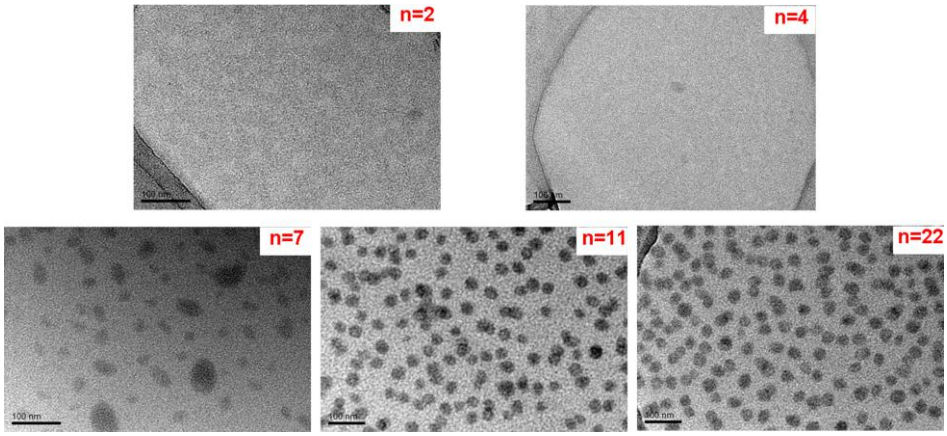

Figure S2. TEM images of $PMMA_{430}$-ec-$PFMA_n$ thin films. Scale bar is 100nm.

Section 4: Chemical composition on $PMMA_{430}$-ec-$PFMA_n$ film surfaces

The surface chemical compositions and properties of the as-cast $PMMA_{430}$-ec-$PFMA_n$ films were characterized by the X-ray photoelectron spectroscopy (XPS) with a photoelectron emission angle of 15° and contact angle measurement. It can be seen from Figure S3 that the surface F/C ratio of fluorinated PMMA films with 7, 12 and 22 FMA units is lower than the F/C ratio of PMMA with 2 and 4 FMA units. Especially for PMMA samples with 12 and 22 FMA units, the F/C ratio approaches

zero and the water contact angle is very close to that of the PMMA homo-polymer [1]. The very low fluorine content of $PMMA_{430}$-ec-$PFMA_{12}$ and $PMMA_{430}$-ec-FMA_{22} films is indicative of the "micelle-like" aggregative structure of chains organized on the surface, with PMMA covering the outermost surface and PFMA buried underneath the micelle corona. However, for PMMA with 2 and 4 FMA units, the PFMA is relatively easier to segregate onto the film surface during spin coating, resulting in higher fluorine content. The surface fluorine content analysis confirms the chain aggregative structure on the film surfaces elucidated by AFM topographies.

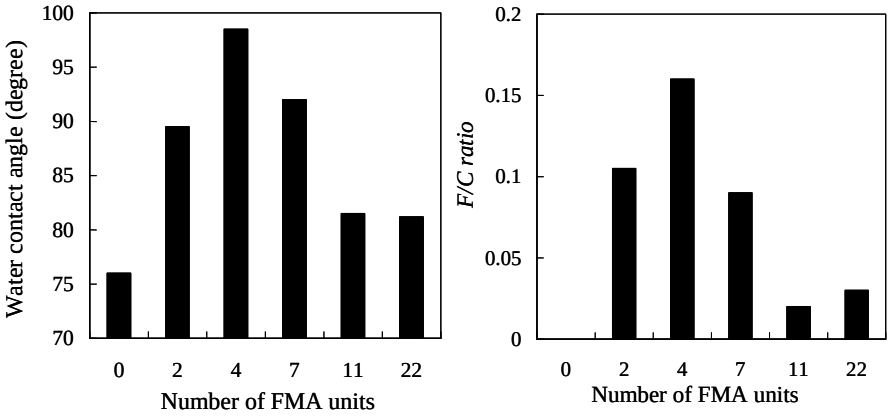

Figure S3. Surface water contact angle (left) and F/C ratio (right) of $PMMA_{430}$-ec-$PFMA_n$ spin-coated films with various numbers of FMA units.

Section 5: Surface fluorine content of $PMMA_{430}$-ec-$PFMA_{22}$ micelle film as function of annealing temperature

Figure S4 displays the XPS curves of $PMMA_{430}$-ec-$PFMA_{22}$ micelle film subjected to various annealing temperatures. When the micelle film is annealed at

76℃, the film surface is almost covered by the PMMA corona of the micelle, with an indiscernible F_{1s} peak in its XPS curve. With increase of the temperature to 85℃, an obvious F_{1s} peak appears in the XPS curve, suggesting that the buried PFMA segments are starting to segregate to the film surface. This temperature for PFMA starting to enrich is in agreement with the onset temperature for PMMA shell opening observed by AFM, which verifies that the opening of the PMMA corona and the enrichment of PFMA are coupled together and the softening of the PMMA corona provides the feasibility in kinetics for the enrichment of PFMA, to retain the thermodynamic requirement of a minimum surface free energy.

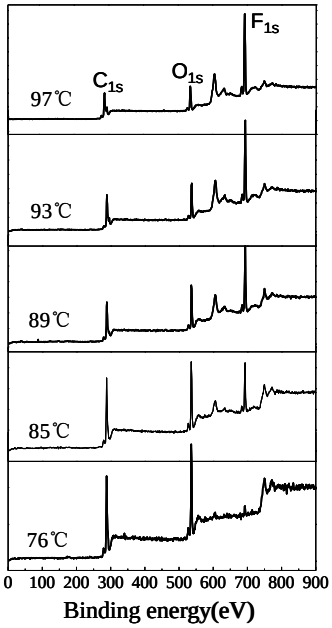

Figure S4. XPS curves of $PMMA_{430}$-ec-$PFMA_{22}$ micelle film annealed at various temperatures (12h).

Section 6: X-ray diffraction of the $PMMA_{430}$-ec-$PFMA_{22}$ micellar film

The micelle film was prepared by casting of 4wt% $PMMA_{430}$-ec-$PFMA_{22}$ toluene solution onto a glass substrate, and then placing in a well-ventilated environment at a temperature of 30 ℃ for rapidly evaporating the toluene to attain a film with thickness of approximately several micrometers composed by dry micelles. The crystallizing of the PFMA core in solid film was analyzed by XRD, as shown in Figure ~~S7~~(S5). It can be seen that the XRD profile only displays a broad peak with 2θ ranging from ~10° to 20°. This broad peak was attributed to an amorphous halo of the PMMA segments. [3] The crystal diffraction peak of PFMA located at 2θ = 6° and 2θ = 17° from the lamellar and hexagonal packing of perfluoroalkyl side chains, respectively [4,5], can not observed in Figure ~~S7~~(S5). This fact indicates that the PFMA segment in the core of micellar film is in an amorphous state, and no observable ordering packing of PFMA segment is evident.

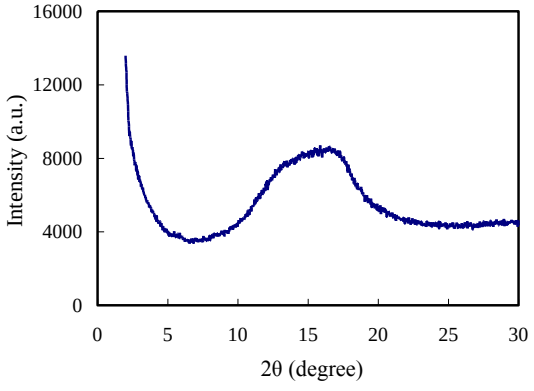

Figure S5. Wide-angle X-ray diffraction (XRD) profile of $PMMA_{430}$-ec-$PFMA_{22}$ micellar film

Section 7: Time evolution of contact angle of the $PMMA_{430}$-ec-$PFMA_{22}$ film annealed at various temperatures

For the micellized PMMA, the films are composed of block polymer micelles, such that the PFMA phase is buried in the center of the micelles. Therefore, it may take a longer time for the chain ends to diffuse to the free surface and this effect may possibly influence the T_R^{onset}. To unveil the role of transport time in the measured T_R^{onset}, we examined the time dependence of PFMA diffusion. Fig. 9 and Fig.~~S8~~ (S6) (**ESI**†) illustrate the time dependence of contact angle for $PMMA_{430}$-ec-$PFMA_2$ and $PMMA_{430}$-ec-$PFMA_{22}$. The result showed that the time scale required to reach an equilibrium surface structure (manifesting as the saturated contact angle) is in the order of 10^1 min for both non-micellized and micellized PMMA, within the temperature range from 85 to 110℃. This time scale for PFMA diffusing is much lower than the annealing time (24h) in our experiment, which indicates that the PFMA

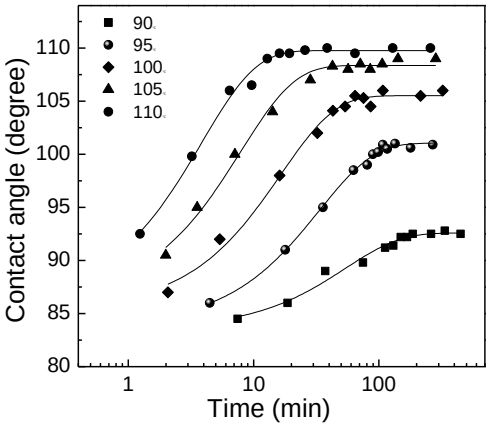

Figure S6. Time evolution of water contact angle of $PMMA_{430}$-ec-$PFMA_{22}$ film annealed at various temperatures.

have long time enough to diffuse to film surface in the annealing process. It is reasonable to exclude the possibility that difference in transport time affect the

measured T_R^{onset}.

Section 8: Apparent activation energy (E_a) determination for surface dynamics of $PMMA_{430}$-ec-$PFMA_n$ (n = 4~22) films

Figure S7 displays the Arrhenius plots of Log α_T vs. temperature for fluorinated PMMA films with 4~22 FMA units. The activation energies for the surface dynamics of PMMA chains with 4, 7, 12, and 22 FMA units are estimated to be 173 KJ/mol, 267 KJ/mol, 310KJ/mol and 317 KJ/mol, respectively, from the slope of the fitted lines.

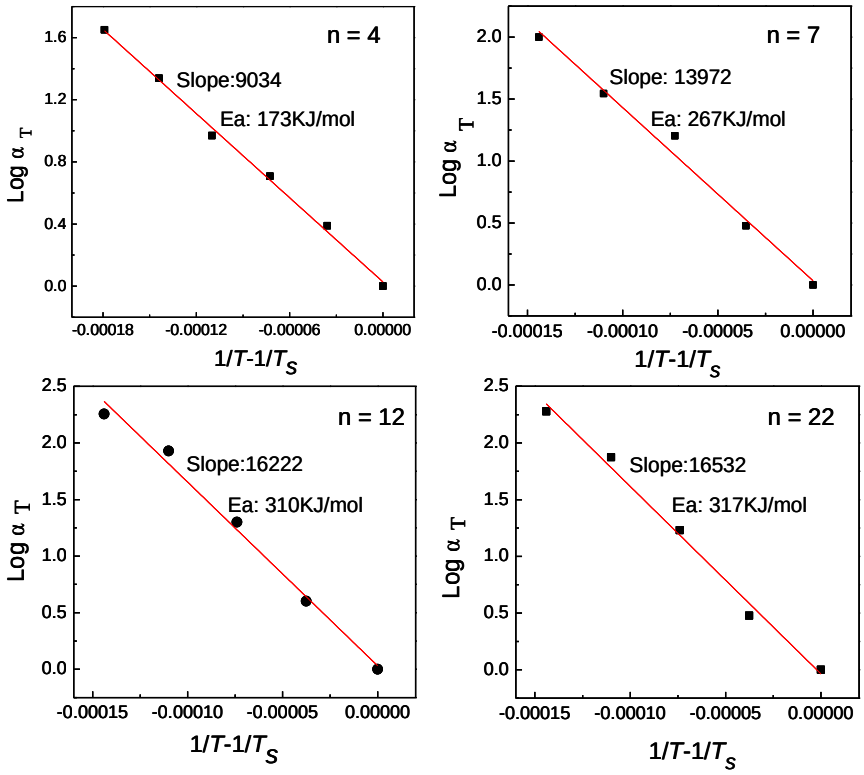

Figure S7. Arrhenius plots of α_T vs. temperature for fluorinated PMMA films with 4~22 FMA units. The solid line is linear least-squares fits by a modified Arrhenius equation described in Eq. 1 to the data with a slope for elucidating the activation energy.

Modified Arrhenius equation:

$$Log\alpha_T = -\frac{E_a}{2.303R}\left(\frac{1}{T}-\frac{1}{T_s}\right) \qquad (1)$$

where R is the gas constant, T_s is the reference temperature, and E_a is the apparent activation energy for surface relaxation.

REFERENCES

(1) X. Y. Ye, B. Zuo, M. Deng, Y. Hei, H. Ni, X. Lu and X. P. Wang, *J. Colloid Interface Sci.,* 2010, **349,** 205-214.

(2) H. J. Busscher, A. W. J. van Pelt, P. de Boer, H. P. de Jong and J. Arends, *Colloids and Surfaces,* 1984, **9,** 319-331.

(3) M. Okouchi, Y. Yamaji and K. Yamauchi, *Macromolecules,* 2006, **39,** 1156-1159.

(4) T. Shimizu, Y. Tanaka, S. Kutsumizu and S. Yano, *Macromolecules*, 1996, **29,** 156-164.

(5) K. Honda, M. Morita, O. Sakata, S. Sasaki and A.Takahara, *Macromolecules,* 2010, **43,** 454-460.